How to cite: *Angew. Chem. Int. Ed.* **2022,** *61,* e202115325
International Edition: doi.org/10.1002/anie.202115325
German Edition: doi.org/10.1002/ange.202115325

Mechanochemistry | Hot Paper

Accelerated Mechanochemistry in Helical Polymers

*Hang Zhang and Charles E. Diesendruck**

Abstract: Polymer chains, if long enough, are known to undergo bond scission when mechanically stressed. While the mechanochemical response of random coils is well understood, biopolymers and some key synthetic chains adopt well-defined secondary structures such as helices. To understand covalent mechanochemistry in such structures, poly(γ-benzyl glutamates) are prepared while regulating the feed-monomer chirality, producing chains with similar molecular weights and backbone chemistry but different helicities. Such chains are stressed in solution and their mechanochemistry rates compared by following molecular weight change and using a rhodamine mechanochromophore. Results reveal that while helicity itself is not affected by the covalent bond scissions, chains with higher helicity undergo faster mechanochemistry. Considering that the polymers tested differ only in conformation, these results indicate that helix-induced chain rigidity improves the efficiency of mechanical energy transduction.

Introduction

Control over polymer chain architecture is a powerful route to tune the mechanical response of materials.[1] Chain morphology influences the molecular arrangement in solution and bulk, affecting how each molecule receives and transmits mechanical energy, as well as the force distribution in the molecule. Among different responses, mechanochemistry,[2] the activation of chemical bonds using mechanical energy, has key consequences to materials' mechanical history, either properties loss[3] or, through the use of mechanophores,[4] the development of mechanoresponsive materials for applications ranging from drug-delivery to self-healing.[5] Therefore, in recent years, numerous efforts have been devoted to understanding the effect of chain architecture on polymer mechanochemistry parameters, especially in solution.[6] For example, using solution ultrasonication, star polymers' mechanochemistry was shown to be governed by their longest linear span, with the additional arms playing no role in the first mechanochemistry cycle.[7] More recently, Peterson et al. systematically investigated architectures which present unfolded backbones due to the presence of large steric hindrance between side chains present in architectures including brush-like and dendronized polymers.[8] In solution ultrasonication, both architectures exhibited mechanochemistry rates proportional to their elongated conformations; however, pronounced differences were measured in the solid state (ball-mill grinding) as a consequence of arm architecture and composition. As one may expect, folding polymer chains has the opposite effect. Cyclic polymers, which become linear after the first scission, presented unusual mechanical response, with fragmented chains partially retaining their original cyclic conformation, rather than becoming elongated as linear chains in solution sonication.[9] Further folding through intramolecular collapse greatly reduces the rate of mechanochemical scission of the polymer into smaller chains, maintaining the polymer properties for longer periods under mechanical stress.[10] Importantly, chains which were covalently folded presented faster rates of mechanochemistry, but scissions occurred at sacrificial intramolecular cross-linkers, preventing chain fragmentation.

Such energy dissipation through sacrificial bonds is very common in natural proteins such as Titin, which contains numerous intramolecular hydrogen bonds that break during chain unfolding prior to stressing covalent bonds in the protein backbone, and can be reformed upon stress release.[11] We have previously shown that this concept also works in synthetic polymers through the creation of intramolecular metal–ligand bonds.[12] Intramolecular covalent disulfide bonds are more common in proteins that are exposed to mechanically aggressive extracellular media, making these sacrificial bonds even more efficient in mechanical energy uptake prior to backbone degradation.[13] In a higher scale, non-covalent interactions can lead to organized domains, such as helices, as a stress-absorbing domain in numerous structural proteins, such as collagen, responsible for skin elasticity.[14] Helicity is also present in several important synthetic polymers such as poly(lactic acid), having profound effects in their thermomechanical properties.[15] This ubiquitous secondary structure should naturally have an effect on the mechanochemical response of covalent macromolecules. Mechanically straining helixes in biopolymers such as DNA and proteins has been carried out using single-molecule force spectroscopy, showing smooth helix-coil transitions in force-extension curves.[16] Herrmann and co-workers recently presented the use of

[*] Dr. H. Zhang, Prof. Dr. C. E. Diesendruck
Schulich Faculty of Chemistry, Technion—Israel Institute of Technology
Haifa 3200008 (Israel)
E-mail: charles@technion.ac.il

ultrasound (US) to control the optical and catalytic activity of genetically engineered green fluorescent protein (GFP), with a structure containing α-helices, β-sheets and disordered sections, but the effect of US in the helix is not clear in this case.[17] Here, poly-γ-benzyl-glutamate, a homopolymer with extremely high degree of helicity, is used as an extreme case to understand the effect of helicity on the rate of backbone polymer mechanochemistry in solution.

Results and Discussion

Poly-γ-benzyl-glutamate (PBG) can be prepared via ring-opening polymerization (ROP) of γ-benzyl-glutamate *N*-carboxyanhydride (NCA) monomers, using LiHMDS as initiator, to provide chains with high molecular weight and low dispersity in one step.[18] PBG, when made using a single enantiomer, forms helical structures in most environments, particularly when having a long-chain length. The level of helicity can be controlled by regulating the chirality of the backbone monomeric unit, with L- and D-type monomers resulting in highly right- or left-handed helical chains, whereas enantiomer mixtures greatly decrease this ordered chain arrangement.[19] Herein, we used the D-, L-type NCAs, and DL-racemic mixtures (D/L ratio, 0.27/0.73, 0.5/0.5) to prepare the four different PBGs (PB(L)G, PB(D)G, PB-($D_{0.27}L_{0.73}$)G, and PB($D_{0.5}L_{0.5}$)G, respectively) with similar degrees of polymerization but different helicities (Scheme 1). Their successful preparation was confirmed by size-exclusion chromatography (SEC) with multi-angle light scattering detector and ^{1}H NMR (see Figures S3 and S6a in the Supporting Information).

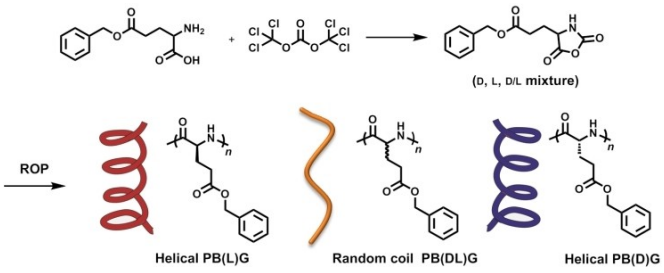

Scheme 1. Preparation of model helical PBGs through ROP.

The helicity of each of the synthesized PBG was determined by circular dichroism (CD) using tetrahydrofuran (THF) as solvent (Figure S8a). The three polymers having excess of one enantiomer, PB(L)G, PB(D)G, PB-($D_{0.27}L_{0.73}$)G, exhibit two peaks at 208 and 222 nm, characteristics of α-helix structures.[18b] In contrast, the PB($D_{0.5}L_{0.5}$)G, made from a racemic mixture, shows no signal in the CD. The helix contents were calculated by the well-established methodology which has been applied in numerous studies of synthetic polypeptides, including PBGs.[20] PB(L)G exhibits the highest helicity (71.5 %), while PB(D)G presents a relatively lower helicity of 63.7 %, probably due to the lower chiral purity of synthetic D-glutamic acid.[20] Notably, PB-(L)G and PB(D)G show opposite signals in the CD, as expected—PB(L)G creating highly right-handed helix and PB(D)G leading to left-handed helical structures. Finally, PB($D_{0.27}L_{0.73}$)G presents 47.3 % helicity (Table 1). These helicities are consistent with the inherent feature of these polypeptides in helicogenic solvents, in which usually imperfect helixes are formed due to non-covalent interactions.[16e] As shown previously, the helicity level increases with enantiomeric excess.[19a,21]

Dilute solutions of the four PBGs (1 mg mL^{-1} in THF) were then subjected to pulsed ultrasonication (1 s on, 2 s off) to assess the effect of solvodynamic shear on their structures. Aliquots were taken every 15 min and analyzed by SEC to record molecular weight changes. Each polymer was independently sonicated and analyzed 3 times for accuracy. In addition, the final solution was also analyzed by CD to check for possible changes in its secondary structure. SEC curves showed clear shifts in the polymer peaks to longer retention time, indicating that all polymers experienced mechanochemical scission in the backbone. However, while tested under the same conditions, the scission behavior was meaningfully different. The SEC curves of both PB(L)G and PB(D)G rapidly and significantly shifted with increasing sonication time, while PB($D_{0.27}$/$L_{0.73}$)G and PB($D_{0.5}$/$L_{0.5}$)G exhibited much smaller changes, presenting only a slight

Table 1: Characterization of polymers used in this study.[a]

Polymer	Feed monomer (ratio)	M_n [kDa][b]	$Đ$[b]	%helix[c]	R_g [nm][b]	Persistence length [nm][d]	Rate constant, k_s [10^{-6} min^{-1}][e]
PB(L)G_{376}	L-NCA	82.3	1.18	71.5	20.0	18.50	9.05 ± 0.02
PB(D)G_{365}	D-NCA	80.0	1.10	63.7	17.0	11.65	6.13 ± 0.09
PB($D_{0.27}L_{0.73}$)G_{388}	D/L (0.27/0.73) NCA	85.0	1.06	47.3	14.5	6.99	4.14 ± 0.03
PB($D_{0.5}L_{0.5}$)G_{332}	D/L (0.5/0.5) NCA	72.7	1.02	0.0	10.4	3.94	2.10 ± 0.05
DAR-PB(L)G_{61}	L-NCA	13.4	1.16	62.9	N.A	N.A	N.A.[f]
DAR-PB($D_{0.5}L_{0.5}$)G_{104}	D/L (0.5/0.5) NCA	22.8	1.04	0.0	N.A	N.A	N.A.
DAR-PB(L)G_{102}	L-NCA	22.3	1.08	58.7	N.A	N.A	N.A.
DAR-PB($D_{0.5}L_{0.5}$)G_{143}	D/L (0.5/0.5) NCA	31.3	1.03	0.0	N.A	N.A	N.A.

[a] Polymers were prepared using LiHMDS or DAR as initiators. [b] Molecular weights (M_n), dispersities ($Đ$), and radius of gyration (R_g) were determined by size-exclusion chromatography (SEC) with multi-angle light scattering (MALS) using DMF (0.02 M of LiBr) as eluent. $Đ$ is underestimated as typical for MALS, but consistent with previous work.[18b] [c] The %helix was determined through CD, using THF as solvent. [d] Calculated from R_g using the worm-like model (see the Supporting Information for details). [e] Calculated from Sato and Nalepa, using the data from three independent sonication experiments.[22] [f] N.A.—not analyzed.

increase in their low molecular weight tails (Figure 1). Using the method developed by Sato and Nalepa,[22] in which the change in number average molecular weight ($1/M_{n,t}-1/M_{n,0}$) is plotted against sonication time, the first-order scission rate constants (k_s) were calculated from the slope (k') of the linear fit (Figure 2a). Interestingly, plotting k_s versus original helical content shows that, even though all polymers have similar degrees of polymerization (DP), the calculated rate constants show significant differences and correlate directly with helicity (Figure 2b). The polymer with the highest helicity, PB(L)G, showed a first-order rate constant which is around four times higher compared to that of a polymer with similar DP but no measurable helicity (PB($D_{0.5}$/$L_{0.5}$)G). Contrary to the observations in randomly folded polymer chains,[10] structured folding in the form of helicity leads to significantly faster mechanochemical degradation of the polymer backbone in solution. CD further demonstrated that the sonicated PBGs have helicity very similar to the unstressed chains, indicating that, in this DP range, shortening the polymer chains through individual mechanochemical scission events does not significantly affect their overall solution conformation (Figure S8b, Table S1).[23]

Given that in all PBGs the backbone chemistry is the same and they all present very similar DPs, the reason

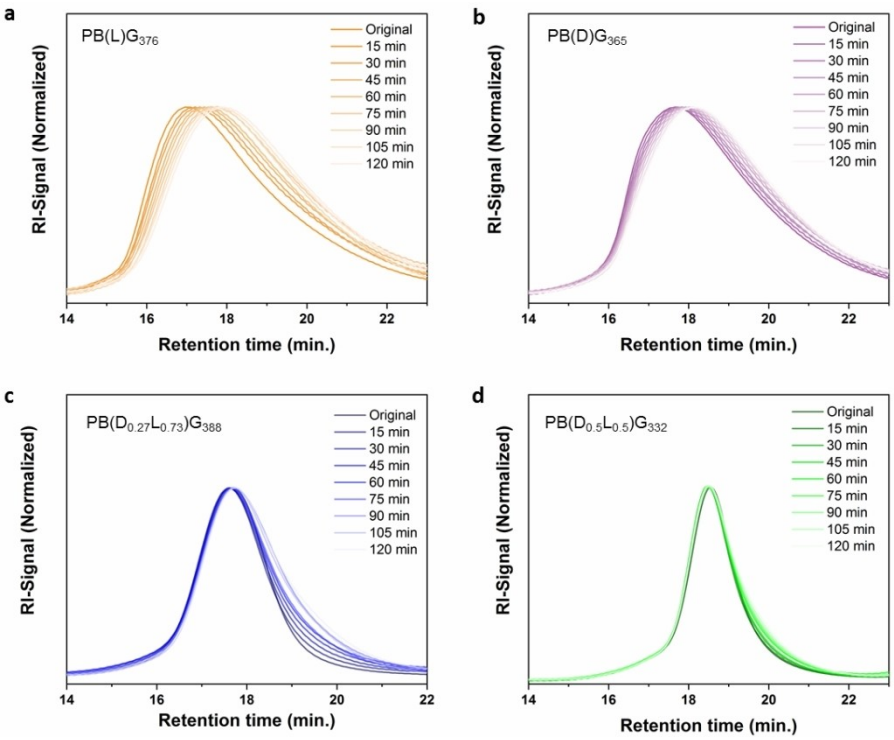

Figure 1. Representative DMF-SEC curves (normalized differential RI signal shown) as a function of sonication time for a) PB(L)G_{376}; b) PB(D)G_{365}; c) PB($D_{0.27}L_{0.73}$)G_{388}; d) PB($D_{0.5}L_{0.5}$)G_{332}.

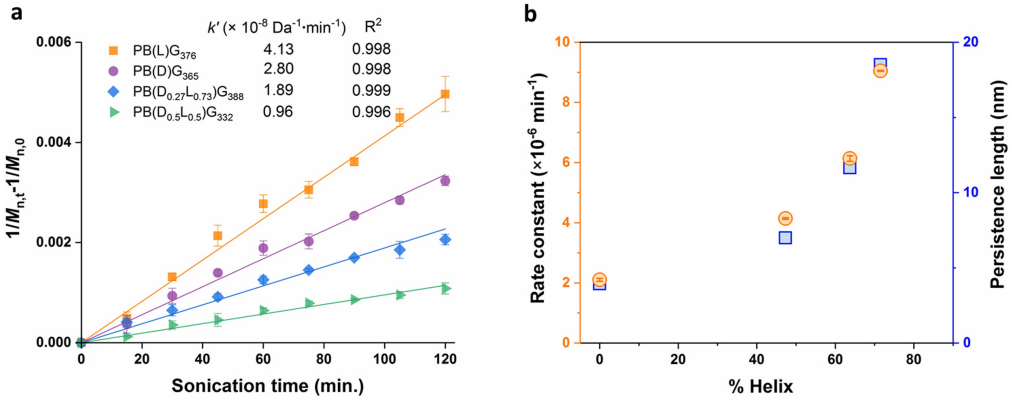

Figure 2. a) Plot of ($1/M_{n,t}-1/M_{n,0}$) versus sonication time, from three independent sonication experiments, including standard deviation, lines are linear fit. b) Mechanochemical rate constants (k_s) and persistence length (l_p) as a function of helical content.

behind this helix-accelerated mechanochemistry needs to be explained by the different solution chain conformation. As previously shown, inclusion of additional intramolecular interactions typically reduce the rate of backbone mechanochemistry, as these act as sacrificial energy sinks during chain unfolding.[24] In single-molecule force microscopy, randomly folded single-chain nanoparticles show protein-like unfolding patterns, with independent "jumps" for each bond scission.[25] Meanwhile PB(L)G shows a uniform unfolding force, presenting a plateau (similar to a multi-mechanophore polymer)[26] when enough strain is applied.[16e] Stressing molecules in solution depends on additional factors. Numerous studies showed that random intramolecular collapse typically leads to a more compact and spherical morphology.[27] Helical chains, on the other hand, adopt extended rod-like conformations, increasing their overall hydrodynamic volume, radius of gyration (as calculated from Zimm plots, see Table 1) and chain stiffness, leading to increased persistence lengths (l_p).[28] This can be easily seen in our measurements as well, as chains with similar DP and higher helicity show shorter retention time in the SEC, even in a less helicogenic solvent like DMF (compared to THF). Peterson et al. has shown that increased persistence length leads to a profound effect on the rate of mechanochemistry in brush-like and dendronized polymers.[29] Clearly it seems like the effect of increased l_p is stronger than that of the presence of intramolecular interactions within the folded chain. To support such concept, the l_p of each PBG chain was calculated from the radius of gyration (R_g) obtained from averaged Zimm-plots done in SEC, using the worm-like model, which has been previously used in natural and synthetic polypeptides (Table 1).[30] PB(L)G_{376}, which has the highest calculated helicity, also presents the longest l_p ~18.5 nm. Meanwhile PB($D_{0.5}$/$L_{0.5}$)G_{332} presents a significantly shorter l_p of 3.94 nm. The relationship between mechanochemistry rate, l_p, and %helix is clearly depicted in Figure 2b.

With these results in mind, one could consider if this helix-accelerating effect can be used towards a constructive response, such as the activation of mechanophores.[2c,31] A morphology change can be used for maintaining a backbone chemistry but creating materials that are more sensitive and efficient in their mechanoresponses. To test this hypothesis, additional PBG chains were prepared having chain-centered rhodamine mechanophores, which provide an optical signal upon mechanical activation. Previous work has demonstrated the stress-responsive feature of spirolactam rhodamine resulted in a molecular isomerization from a twisted form to a zwitterionic planarized ring-open state, causing a significant red-shift in the absorption band.[32] The same strategy of controlling the chirality of feeding monomers was employed to regulate the helicity of the rhodamine-containing PBG chains. Following the previously demonstrated strategy of using the mechanophore as a di-initiators in controlled polymerization, the spirolactam rhodamine could be perfectly tethered in the center of the PBG chains in helical or random conformations (Figure 3a). To combine this mechanophore into PBG ROP chemistry, a new diamine-functionalized spirolactam rhodamine (DAR), was designed and synthesized (Scheme S1, Figure S2) on the basis of previously reported dihydroxyl functionalized rhodamine (DHR).[32b]

DAR was used to polymerize NCAs (L- or DL-type) at 0 °C in anhydrous DMF, providing four additional PBGs with different lengths and helicities: DAR-PB(L)G_{61}, DAR-PB(L)G_{102}, DAR-PB($D_{0.5}L_{0.5}$)G_{104} and DAR-PB-($D_{0.5}L_{0.5}$)G_{143}, respectively (Table 1, Figure S6b). ^{1}H NMR was used to confirm the polymer structure, as well as the presence of the characteristic signals of rhodamine (Figures S4, S5). CD confirmed that the two polymers made using only the L-enantiomer present high helicities in THF (62.9

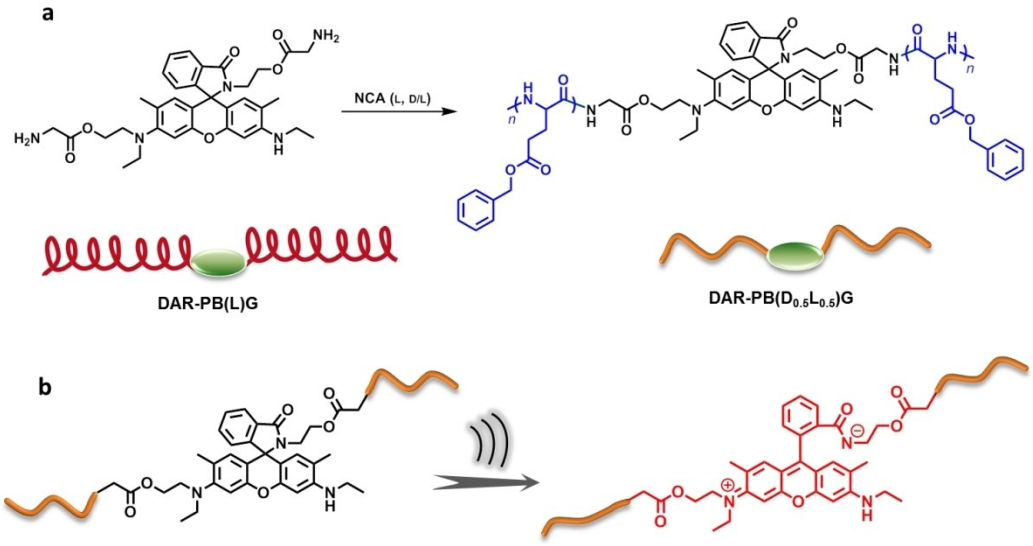

Figure 3. a) Synthesis of PBG chains with chain-centered rhodamine mechanophores, having helical or random coil chains. b) Schematic mechanochemical rhodamine under shear forces from solvodynamic shear.

and 58.7 % for DAR-PB(L)G_{61}, DAR-PB(L)G_{102}, respectively), while the two DAR-PB($D_{0.5}L_{0.5}$)Gs made from monomer racemic mixture presented no helicity (Figure S8c).

As before, these new rhodamine-containing PBGs were subjected to pulsed ultrasonication, with aliquots being taken every hour and immediately analyzed by UV/Vis to assess the rhodamine mechanochemical activation. As expected, the rhodamine mechanophore within all PBG chains could be activated, clearly seen by the color change in the polymer solutions from colorless to light pink (Figure 3b and Figure 4a). A characteristic absorption peak at 538 nm appeared and increased with sonication time (Figures S9, S10). Importantly, no meaningful changes in the SECs are seen (Figure S7), given these chains are quite short; however, significant differences in activation rates of rhodamine were found (Figure 4b). Considering the two DAR-PBGs with equivalent chain length, DAR-PB(L)G_{102} and DAR-PB($D_{0.5}L_{0.5}$)G_{104}, the highly helical version presented almost four times higher rhodamine activation. Moreover, it showed higher activation even when compared to DAR-PB($D_{0.5}L_{0.5}$)G_{143}, which has ca. 40 % higher DP but no measurable helicity.[33] This observation is also seen in a smaller helical chain, DAR-PB(L)G_{61}, which presented about twice higher rhodamine activation compared to the non-helical DAR-PB($D_{0.5}L_{0.5}$)G_{104} which has almost twice the DP. Such mechanophore activation difference between helical and random coil PBG chains agrees well with the above-demonstrated helix-accelerated mechanochemistry, and strongly supports that chains with helical conformation are more efficient in mechanochemical transduction.

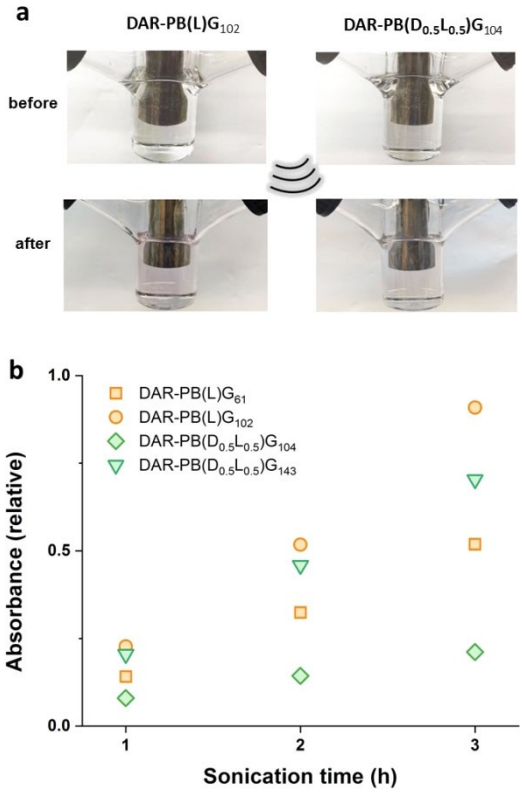

Figure 4. a) The color contrast of DAR-PB(L)G_{102} and DAR-PB-($D_{0.5}L_{0.5}$)G_{104} solutions before and after sonication. b) The normalized absorbance (at 538 nm) of helical DAR-PB(L)Gs and random coil DAR-PB($D_{0.5}L_{0.5}$)Gs with the sonication time.

Conclusion

To conclude, we studied the effect of helicity on the rate of polymer mechanochemistry in solution. Poly(γ-benzyl glutamates) with different helicities, used as model polymers, demonstrated that chains with the higher helicity exhibit higher mechanochemical rate constants, be it backbone fragmentation or mechanophore activation, with a clear correlation seen between helicity and rate constant. Given the study was done in chains with similar chemical compositions and degrees of polymerization, this result is attributed to the increased l_p in the elongated rod-like conformation of helical polymers, leading to more efficient energy transduction and a morphology which is more easily oriented towards the force vector.[8,29] Furthermore, we have shown that helix can be used as an efficient morphological change to increase the response of rhodamine mechanophores without increasing (and even in smaller) degrees of polymerization, expanding the strategies to develop efficient mechanoresponsive materials based on synthetic or semi-synthetic polymers.

Acknowledgements

The authors acknowledge the Israel Science Foundation (Grant No. 354/19) for financial support. The authors also thank Anastasia Behar, Diana Blumenthal, and Prof. Galia Maayan for support with CD spectroscopy.

Conflict of Interest

The authors declare no conflict of interest.

Data Availability Statement

The data that support the findings of this study are available in the Supporting Information of this article.

Keywords: Helical Conformation · Mechanochemistry · Mechanophore · Polypeptides · Stress-Response

[1] a) L. Montero de Espinosa, W. Meesorn, D. Moatsou, C. Weder, *Chem. Rev.* **2017**, *117*, 12851–12892; b) O. Galant, S. Bae, M. N. Silberstein, C. E. Diesendruck, *Adv. Funct. Mater.* **2020**, *30*, 1901806.

[2] a) M. M. Caruso, D. A. Davis, Q. Shen, S. A. Odom, N. R. Sottos, S. R. White, J. S. Moore, *Chem. Rev.* **2009**, *109*, 5755–5798; b) J. Li, C. Nagamani, J. S. Moore, *Acc. Chem. Res.* **2015**, *48*, 2181–2190; c) M. A. Ghanem, A. Basu, R. Behrou, N.

Boechler, A. J. Boydston, S. L. Craig, Y. Lin, B. E. Lynde, A. Nelson, H. Shen, D. W. Storti, *Nat. Rev. Mater.* **2021**, *6*, 84–98; d) R. T. O'Neill, R. Boulatov, *Nat. Chem. Rev.* **2021**, *5*, 148–167.

[3] S. Aharonovich, C. E. Diesendruck, *React. Funct. Polym.* **2018**, *131*, 237–242.

[4] a) P. A. May, J. S. Moore, *Chem. Soc. Rev.* **2013**, *42*, 7497–7506; b) G. De Bo, *Macromolecules* **2020**, *53*, 7615–7617; c) N. Willis-Fox, E. Rognin, T. A. Aljohani, R. Daly, *Chem* **2018**, *4*, 2499–2537.

[5] a) C. E. Diesendruck, N. R. Sottos, J. S. Moore, S. R. White, *Angew. Chem. Int. Ed.* **2015**, *54*, 10428–10447; *Angew. Chem.* **2015**, *127*, 10572–10593; b) Z. Shi, Q. Song, R. Gostl, A. Herrmann, *Chem. Sci.* **2021**, *12*, 1668–1674; c) Z. Shi, J. Wu, Q. Song, R. Gostl, A. Herrmann, *J. Am. Chem. Soc.* **2020**, *142*, 14725–14732; d) S. Huo, P. Zhao, Z. Shi, M. Zou, X. Yang, E. Warszawik, M. Loznik, R. Gostl, A. Herrmann, *Nat. Chem.* **2021**, *13*, 131–139; e) Y. Chen, G. Mellot, D. van Luijk, C. Creton, R. P. Sijbesma, *Chem. Soc. Rev.* **2021**, *50*, 4100–4140.

[6] a) H. Zhang, Y. Lin, Y. Xu, W. Weng, in *Polymer Mechanochemistry, Vol. 369* (Eds.: R. Boulatov), Springer International Publishing, Chem, **2015**, pp. 135–207; b) G. I. Peterson, T. L. Choi, *Chem. Commun.* **2021**, *57*, 6465–6474.

[7] D. C. Church, G. I. Peterson, A. J. Boydston, *ACS Macro Lett.* **2014**, *3*, 648–651.

[8] J. Noh, G. I. Peterson, T.-L. Choi, *Angew. Chem. Int. Ed.* **2021**, *60*, 18651–18659; *Angew. Chem.* **2021**, *133*, 18799–18807.

[9] Y. Lin, Y. Zhang, Z. Wang, S. L. Craig, *J. Am. Chem. Soc.* **2019**, *141*, 10943–10947.

[10] a) F. Wang, C. E. Diesendruck, *Chem. Commun.* **2020**, *56*, 2143–2146; b) A. Levy, E. Gaver, F. Wang, O. Galant, C. E. Diesendruck, *Chem. Commun.* **2017**, *53*, 10132–10135; c) A. Levy, F. Wang, A. Lang, O. Galant, C. E. Diesendruck, *Angew. Chem. Int. Ed.* **2017**, *56*, 6431–6434; *Angew. Chem.* **2017**, *129*, 6531–6534.

[11] C. A. Opitz, M. Kulke, M. C. Leake, C. Neagoe, H. Hinssen, R. J. Hajjar, W. A. Linke, *Proc. Natl. Acad. Sci. USA* **2003**, *100*, 12688.

[12] A. Levy, R. Feinstein, C. E. Diesendruck, *J. Am. Chem. Soc.* **2019**, *141*, 7256–7260.

[13] J. S. Wall, *J. Agric. Food Chem.* **1971**, *19*, 619–625.

[14] M. D. Shoulders, R. T. Raines, *Annu. Rev. Biochem.* **2009**, *78*, 929–958.

[15] a) S. Sasaki, T. Asakura, *Macromolecules* **2003**, *36*, 8385–8390; b) K. Aou, S. Kang, S. L. Hsu, *Macromolecules* **2005**, *38*, 7730–7735; c) J. Hughes, R. Thomas, Y. Byun, S. Whiteside, *Carbohydr. Polym.* **2012**, *88*, 165–172.

[16] a) R. Afrin, I. Takahashi, K. Shiga, A. Ikai, *Biophys. J.* **2009**, *96*, 1105–1114; b) A. Janshoff, M. Neitzert, Y. Oberdörfer, H. Fuchs, *Angew. Chem. Int. Ed.* **2000**, *39*, 3212–3237; *Angew. Chem.* **2000**, *112*, 3346–3374; c) M. Kageshima, M. A. Lantz, S. P. Jarvis, H. Tokumoto, S. Takeda, A. Ptak, C. Nakamura, J. Miyake, *Chem. Phys. Lett.* **2001**, *343*, 77–82; d) H. Clausen-Schaumann, M. Rief, C. Tolksdorf, H. E. Gaub, *Biophys. J.* **2000**, *78*, 1997–2007; e) D. Sluysmans, N. Willet, J. Thevenot, S. Lecommandoux, A. S. Duwez, *Nanoscale Horiz.* **2020**, *5*, 671–678; f) F. Berkemeier, M. Bertz, S. Xiao, N. Pinotsis, M. Wilmanns, F. Gräter, M. Rief, *Proc. Natl. Acad. Sci. USA* **2011**, *108*, 14139.

[17] Y. Zhou, S. Huo, M. Loznik, R. Göstl, A. J. Boersma, A. Herrmann, *Angew. Chem. Int. Ed.* **2021**, *60*, 1493–1497; *Angew. Chem.* **2021**, *133*, 1515–1519.

[18] a) M. Li, S. Zhang, X. Zhang, Y. Wang, J. Chen, Y. Tao, X. Wang, *Angew. Chem. Int. Ed.* **2021**, *60*, 6003–6012; *Angew. Chem.* **2021**, *133*, 6068–6077; b) Y. Wu, D. Zhang, P. Ma, R. Zhou, L. Hua, R. Liu, *Nat. Commun.* **2018**, *9*, 5297.

[19] a) H. Yao, K. Sheng, J. Sun, S. Yan, Y. Hou, H. Lu, B. D. Olsen, *Polym. Chem.* **2020**, *11*, 3032–3045; b) C. Zhang, J. Yuan, J. Lu, Y. Hou, W. Xiong, H. Lu, *Biomaterials* **2018**, *178*, 728–737; c) M. Li, Y. Tao, J. Tang, Y. Wang, X. Zhang, Y. Tao, X. Wang, *J. Am. Chem. Soc.* **2019**, *141*, 281–289.

[20] C. Chen, Z. Wang, Z. Li, *Biomacromolecules* **2011**, *12*, 2859–2863.

[21] S. Kitazawa, T. Hiraoki, A. Tsutsumi, *J. Mol. Struct.* **1995**, *355*, 87–94.

[22] T. Sato, D. E. Nalepa, *J. Appl. Polym. Sci.* **1978**, *22*, 865–867.

[23] S. G. Ostlund, A. M. Striegel, *Polym. Degrad. Stab.* **2008**, *93*, 1510–1514.

[24] A. Levy, H. Goldstein, D. Brenman, C. E. Diesendruck, *J. Polym. Sci.* **2020**, *58*, 692–703.

[25] N. Hosono, A. M. Kushner, J. Chung, A. R. A. Palmans, Z. Guan, E. W. Meijer, *J. Am. Chem. Soc.* **2015**, *137*, 6880–6888.

[26] M. H. Barbee, T. Kouznetsova, S. L. Barrett, G. R. Gossweiler, Y. Lin, S. K. Rastogi, W. J. Brittain, S. L. Craig, *J. Am. Chem. Soc.* **2018**, *140*, 12746–12750.

[27] a) J. Chen, E. S. Garcia, S. C. Zimmerman, *Acc. Chem. Res.* **2020**, *53*, 1244–1256; b) R. Chen, E. B. Berda, *ACS Macro Lett.* **2020**, *9*, 1836–1843; c) E. Verde-Sesto, A. Arbe, A. J. Moreno, D. Cangialosi, A. Alegría, J. Colmenero, J. A. Pomposo, *Mater. Horiz.* **2020**, *7*, 2292–2313.

[28] P. Doty, J. H. Bradbury, A. M. Holtzer, *J. Am. Chem. Soc.* **1956**, *78*, 947–954.

[29] a) G. I. Peterson, J. Noh, K.-T. Bang, H. Ma, K. T. Kim, T.-L. Choi, *Macromolecules* **2020**, *53*, 1623–1628; b) G. I. Peterson, K. T. Bang, T. L. Choi, *J. Am. Chem. Soc.* **2018**, *140*, 8599–8608.

[30] a) A. M. Rosales, H. K. Murnen, S. R. Kline, R. N. Zuckermann, R. A. Segalman, *Soft Matter* **2012**, *8*, 3673; b) H. Gu, Y. Nakamura, T. Sato, A. Teramoto, M. M. Green, C. Andreola, *Polymer* **1999**, *40*, 849–856.

[31] a) A. L. Black, J. M. Lenhardt, S. L. Craig, *J. Mater. Chem.* **2011**, *21*, 1655–1663; b) H. Qian, N. S. Purwanto, D. G. Ivanoff, A. J. Halmes, N. R. Sottos, J. S. Moore, *Chem* **2021**, *7*, 1080–1091; c) J. M. Lenhardt, A. L. Black Ramirez, B. Lee, T. B. Kouznetsova, S. L. Craig, *Macromolecules* **2015**, *48*, 6396–6403.

[32] a) Z. Wang, Z. Ma, Y. Wang, Z. Xu, Y. Luo, Y. Wei, X. Jia, *Adv. Mater.* **2015**, *27*, 6469–6474; b) T. Wang, N. Zhang, J. Dai, Z. Li, W. Bai, R. Bai, *ACS Appl. Mater. Interfaces* **2017**, *9*, 11874–11881.

[33] P. A. May, N. F. Munaretto, M. B. Hamoy, M. J. Robb, J. S. Moore, *ACS Macro Lett.* **2016**, *5*, 177–180.

Manuscript received: November 11, 2021
Accepted manuscript online: January 24, 2022
Version of record online: February 3, 2022